



Periodic forced convection with axial heat conduction in a circular duct

A. Barletta*, E. Rossi di Schio

Dipartimento di Ingegneria Energetica, Nucleare e del Controllo Ambientale (DIENCA), Università di Bologna, Viale Risorgimento 2, I-40136 Bologna, Italy

Received 22 March 1999; received in revised form 29 September 1999

Abstract

Stationary and laminar forced convection in a circular duct is analyzed in the case of a sinusoidal axial change of the wall heat flux such that the modulus of its mean value is either zero or equal to the amplitude. The effect of the axial heat conduction in the fluid is taken into account. Reference is made to the thermally developed region where the temperature distribution can be expressed as the sum of a linear function and a periodic function of the axial coordinate. The temperature field as well as the local and mean Nusselt numbers are evaluated analytically. Comparisons with the solution in the absence of axial heat conduction are performed. © 2000 Elsevier Science Ltd. All rights reserved.

Keywords: Forced convection; Laminar flow; Axial heat conduction; Analytical method

1. Introduction

The interest deserved to the subject of laminar forced convection in circular ducts is mainly due to its importance in many technological applications which range from heat exchangers to solar collectors. The most important results available in the literature are outlined in review papers of Shah and London [1], Kays and Perkins [2], Shah and Bhatti [3].

The effect of the axial heat conduction in the fluid has been investigated in many papers which refer to different kinds of boundary conditions. It is well known that, when the Peclet number is small, the axial

heat conduction in the fluid becomes relevant. Then, this effect can be very important for fluids with a small Prandtl number as, for instance, liquid metals.

Analytical solutions of the local energy balance equation by taking into account the effect of axial heat conduction in the fluid have been obtained by Soliman [4], Ebdian and Zhang [5,6], Yin and Bau [7] and Olek [8]. Soliman [4] considers a slug flow within a circular duct, which is heated over a finite length with a uniform wall heat flux and is externally insulated both upstream and downstream of the heated region. Plots of the dimensionless heat flux, bulk temperature, wall temperature as well as of the Nusselt number versus the dimensionless axial coordinate are reported. Axial conduction both in the wall and in the fluid is taken into account, and all the plots are drawn for two different values of the Peclet number: $Pe = 5$ and 50 . In Refs. [5,6], the Fourier transform method is employed in order

* Corresponding author. Tel.: +39-051-2093295; fax: +39-051-2093296.

E-mail address: antonio.barletta@mail.ing.unibo.it (A. Barletta).

Nomenclature

| | |
|-----------------|--|
| a | complex dimensionless parameter, = $(1 - \omega A)/2$ |
| B | dimensionless parameter, = $2r_0 Pe \beta$ |
| C_0 | constant introduced in Eq. (16) |
| ${}_1F_1$ | confluent hypergeometric function |
| ${}_1F_1'$ | derivative of the confluent hypergeometric function, given by Eq. (31) |
| $G(a, \omega)$ | integration constant introduced in Eq. (27) |
| h | local convection coefficient, = $q_w/(T_w - T_m)$ (W/(m ² K)) |
| i | imaginary unit, = $\sqrt{-1}$ |
| k | thermal conductivity (W/(m K)) |
| L | constant such that $x = -L$ is the inlet section of the pipe (m) |
| n | non-negative integer |
| Nu | Nusselt number, = $2r_0 q_w/[k(T_w - T_m)]$ |
| \overline{Nu} | mean value of Nu in an axial period |
| Pe | Peclet number, = $2r_0 \bar{u}/\alpha$ |
| q_w | wall heat flux (W/m ²) |
| q_0 | constant introduced in Eq. (1) (W/m ²) |
| r | radial coordinate (m) |
| r_0 | radius of the pipe (m) |
| s, t | complex dimensionless parameters |
| T | temperature (K) |
| T_e | inlet temperature (K) |
| u | velocity component in the axial direction (m/s) |
| \bar{u} | mean value of u (m/s) |
| x | axial coordinate (m) |
| z | complex variable |

Greek symbols

| | |
|---|---|
| α | thermal diffusivity (m ² /s) |
| β | constant defined by Eq. (1) (m ⁻¹) |
| γ | dimensionless parameter defined by Eq. (1) |
| Γ | Euler's gamma function |
| η | dimensionless radius, = r/r_0 |
| ϑ | dimensionless temperature, = $k(T - T_e)/(r_0 q_0)$ |
| $\vartheta_0, \vartheta_1, \vartheta_2$ | dimensionless functions defined by Eq. (8) |
| A | dimensionless complex parameter, = $1 - iB/(2Pe^2)$ |
| μ | dynamic viscosity (Pa s) |
| ν | kinematic viscosity, = μ/ρ (m ² /s) |
| ξ | dimensionless axial coordinate, = $x/(2r_0 Pe)$ |
| ξ_e | dimensionless axial position of the inlet section, = $-L/(2r_0 Pe)$ |
| ξ_n | dimensionless constant defined in Eq. (40) |
| ρ | mass density (kg/m ³) |
| ψ | dimensionless function, = $\vartheta_1 + i\vartheta_2$ |
| ω | dimensionless complex parameter, = $\sqrt{-iB/8}$ |

Subscripts

| | |
|---|---|
| m | mixing-cup quantity defined by Eq. (17) |
| w | quantity evaluated at the wall |

to evaluate analytically the mixed mean temperature, the heat flux and the Nusselt number for a boundary condition given by a step change of the wall temperature. These quantities are then plotted against the axial coordinate for different values of the Peclet number (varying from 3 to 150). Moreover, in Ref. [6], the effects of a heat generation within the fluid are taken into account and plots of the mean Nusselt number versus the heat generation number for different values of Pe (in the range from 0.5 to 10) are reported. Yin and Bau [7] consider both Poiseuille flow and slug flow in a duct with boundary conditions of either uniform wall temperature or uniform wall heat flux. In Ref. [8], an eigenfunction expansion is used to derive a solution of the energy equation for a non-Newtonian fluid, with boundary conditions of either uniform wall temperature or external convection.

Numerical solutions, based on the finite difference method, have been recently developed by Fahgri et al.

[9], Nguyen [10] and Bilir [11,12]. Fahgri et al. [9] investigate a conjugate heat transfer problem, by considering an internal flow with blowing or suction in a duct with a porous wall. Plots of the temperature, the heat flux and the Nusselt number at the internal surface of the wall are drawn against the axial coordinate for two different values of the Peclet number, i.e. $Pe = 100$ and 1000 . Nguyen [10] considers boundary conditions given by a step change either of the wall temperature or of the wall heat flux. In the case of prescribed wall heat flux, the author reports a table of the local and fully developed Nusselt numbers for different values of the Peclet number. In Ref. [11], the thermal entrance region is investigated with two different boundary conditions: (1) a step change of the wall temperature; (2) a step change of the wall heat flux. In the case of prescribed wall heat flux, plots of the local Nusselt number are drawn against the axial coordinate for different values of Pe (varying from 1 to 50). In Ref. [12], a step change of temperature at the external

surface of the wall is considered and axial heat conduction is supposed to be present both in the fluid and in the wall. Three different values for the Peclet numbers are considered: $Pe = 1, 5$ and 20 . The bulk temperature and the local Nusselt number, as well as the wall heat flux and the wall temperature evaluated at the interface between solid and fluid, are plotted against the axial coordinate.

The boundary condition of axially varying wall heat flux has been considered in Refs. [13] and [14]. Pearlstein and Dempsey [13] plot both the bulk temperature and the temperature distribution in the thermal entrance region, for various Peclet numbers. These authors refer to wall heat fluxes which undergo an axial variation given either by a sinusoidal distribution or by a hyperbolic tangent distribution. In Ref. [14], a boundary heat flux which changes axially with an exponential law is considered and the fully developed Nusselt number is determined analytically.

For engineering applications, it is well known that periodic axial changes of wall heat flux are of great technical interest as, for instance, in the design of cooling tubes for nuclear reactors and in the analysis of heat transfer in the heat exchangers of Stirling-cycle machines. Boundary conditions of this kind have been employed in Ref. [15] and represent the simplest kind of axially periodic heating or cooling. Ref. [15] deals with the behavior at a sufficiently great distance from the inlet section. In this region, forced convection is hydrodynamically developed and the temperature distribution can be expressed as the sum of a linear function and a periodic function of the axial coordinate.

The aim of the present paper is an improvement of the analysis presented in Ref. [15] in order to take into account the effect of axial heat conduction in the fluid. The laminar forced convection in a circular duct is investigated in the case of a sinusoidal axial variation of the wall heat flux. The energy equation is solved analytically and expressions of the temperature field as well as of the local and mean Nusselt numbers are obtained in terms of the confluent hypergeometric function.

2. Governing equations

In this section, the energy equation together with its boundary condition given by a sinusoidal heat flux distribution are written in a dimensionless form and solved analytically.

Let us consider an infinitely long circular duct with radius r_0 crossed by a Newtonian fluid such that its thermal conductivity k , dynamic viscosity μ and thermal diffusivity α can be treated as constants. A regime of laminar and fully developed forced convection is

assumed. The effect of viscous dissipation is considered as negligible, while the axial heat conduction in the fluid is taken into account.

Let us assume that a sinusoidal axial variation of the heat flux density is present at the duct wall, namely

$$q_w(x) = q_0[\gamma + \sin(\beta x)], \tag{1}$$

where γ is a dimensionless parameter which can be either 0 or 1. If $\gamma = 1$, Eq. (1) yields a periodic wall heat flux distribution such that the amplitude of the oscillations coincides with the modulus of its mean value. This case corresponds either to fluid heating or to fluid cooling, depending on the sign of the constant q_0 . On the other hand, if $\gamma = 0$, both for $q_0 > 0$ and $q_0 < 0$, the wall heat flux distribution has a vanishing mean value.

At the inlet of the pipe, which is placed at $x = -L$, the temperature is supposed to be uniform with value T_e .

In the region of hydrodynamically developed flow, the energy equation can be written as

$$\frac{\partial}{\partial r} \left(r \frac{\partial T}{\partial r} \right) + r \frac{\partial^2 T}{\partial x^2} - \frac{u(r)r}{\alpha} \frac{\partial T}{\partial x} = 0, \tag{2}$$

where $u(r)$ is the fluid velocity distribution, given by the well known Hagen–Poiseuille expression:

$$u(r) = 2\bar{u} \left[1 - \left(\frac{r}{r_0} \right)^2 \right]. \tag{3}$$

By introducing the dimensionless temperature $\vartheta = k(T - T_e)/(q_0 r_0)$, the Peclet number $Pe = 2r_0 \bar{u}/\alpha$, the dimensionless radius $\eta = r/r_0$ and the dimensionless axial coordinate $\xi = x/(2r_0 Pe)$, Eq. (2) can be rewritten in the dimensionless form

$$\frac{\partial}{\partial \eta} \left(\eta \frac{\partial \vartheta}{\partial \eta} \right) + \frac{\eta}{4Pe^2} \frac{\partial^2 \vartheta}{\partial \xi^2} - \frac{1}{2} \eta (1 - \eta^2) \frac{\partial \vartheta}{\partial \xi} = 0. \tag{4}$$

As it is shown by Eq. (4), the effect of the axial heat conduction in the fluid becomes relevant only if the Peclet number is sufficiently small. The condition of negligible axial conduction corresponds to the limit $Pe \rightarrow \infty$.

The boundary condition on temperature is as follows:

$$k \frac{\partial T}{\partial r} \Big|_{r=r_0} = q_w(x). \tag{5}$$

If the boundary heat flux is expressed by Eq. (1), Eq. (5) can be rewritten as

$$\frac{\partial \vartheta}{\partial \eta} \Big|_{\eta=1} = \gamma + \sin(B\xi), \tag{6}$$

where the dimensionless parameter $B = 2r_0Pe\beta$ is employed. Moreover, the following symmetry condition at $\eta = 0$ is required:

$$\left. \frac{\partial \vartheta}{\partial \eta} \right|_{\eta=0} = 0. \quad (7)$$

At axial positions sufficiently distant from the inlet section of the tube, the solution of Eq. (4) can be written as

$$\begin{aligned} \vartheta(\eta, \xi) = & 8\gamma\xi + \vartheta_0(\eta) + \vartheta_1(\eta)\sin(B\xi) \\ & + \vartheta_2(\eta)\cos(B\xi), \end{aligned} \quad (8)$$

where the functions $\vartheta_0(\eta)$, $\vartheta_1(\eta)$ and $\vartheta_2(\eta)$ can be determined by substituting Eq. (8) into Eqs. (4), (6) and (7). In fact, Eqs. (4), (6) and (7) yield

$$\begin{aligned} & \frac{d}{d\eta} \left(\eta \frac{d\vartheta_0}{d\eta} \right) - 4\gamma\eta(1 - \eta^2) \\ & + \left[\frac{d}{d\eta} \left(\eta \frac{d\vartheta_1}{d\eta} \right) + \frac{B}{2}\eta(1 - \eta^2)\vartheta_2 - \frac{B^2}{4Pe^2}\eta\vartheta_1 \right] \\ & \times \sin(B\xi) + \left[\frac{d}{d\eta} \left(\eta \frac{d\vartheta_2}{d\eta} \right) - \frac{B}{2}\eta(1 - \eta^2)\vartheta_1 - \frac{B^2}{4Pe^2}\eta\vartheta_2 \right] \\ & \times \cos(B\xi) = 0, \end{aligned} \quad (9)$$

$$\left. \frac{d\vartheta_0}{d\eta} \right|_{\eta=1} + \left[\left. \frac{d\vartheta_1}{d\eta} \right|_{\eta=1} - 1 \right] \sin(B\xi) + \left. \frac{d\vartheta_2}{d\eta} \right|_{\eta=1} \cos(B\xi) = \gamma, \quad (10)$$

$$\left. \frac{d\vartheta_0}{d\eta} \right|_{\eta=0} + \left. \frac{d\vartheta_1}{d\eta} \right|_{\eta=0} \sin(B\xi) + \left. \frac{d\vartheta_2}{d\eta} \right|_{\eta=0} \cos(B\xi) = 0. \quad (11)$$

Eqs. (9)–(11) can be integrated with respect to ξ in the interval $[0, 2\pi/B]$ and yield

$$\frac{d}{d\eta} \left(\eta \frac{d\vartheta_0}{d\eta} \right) - 4\gamma\eta(1 - \eta^2) = 0,$$

$$\left. \frac{d\vartheta_0}{d\eta} \right|_{\eta=1} = \gamma, \quad \left. \frac{d\vartheta_0}{d\eta} \right|_{\eta=0} = 0. \quad (12)$$

By multiplying both sides of Eqs. (9)–(11) by $\sin(B\xi)$ and by integrating with respect to ξ in the interval $[0, 2\pi/B]$, one obtains

$$\frac{d}{d\eta} \left(\eta \frac{d\vartheta_1}{d\eta} \right) + \frac{B}{2}\eta(1 - \eta^2)\vartheta_2 - \frac{B^2}{4Pe^2}\eta\vartheta_1 = 0,$$

$$\left. \frac{d\vartheta_1}{d\eta} \right|_{\eta=1} = 1, \quad \left. \frac{d\vartheta_1}{d\eta} \right|_{\eta=0} = 0. \quad (13)$$

Finally, by multiplying both sides of Eqs. (9)–(11) by $\cos(B\xi)$ and by integrating with respect to ξ in the interval $[0, 2\pi/B]$, one obtains

$$\frac{d}{d\eta} \left(\eta \frac{d\vartheta_2}{d\eta} \right) - \frac{B}{2}\eta(1 - \eta^2)\vartheta_1 - \frac{B^2}{4Pe^2}\eta\vartheta_2 = 0,$$

$$\left. \frac{d\vartheta_2}{d\eta} \right|_{\eta=1} = 0, \quad \left. \frac{d\vartheta_2}{d\eta} \right|_{\eta=0} = 0. \quad (14)$$

If one introduces the complex valued function $\psi(\eta) = \vartheta_1(\eta) + i\vartheta_2(\eta)$, Eqs. (13) and (14) can be collapsed into a unique boundary value problem, namely

$$\frac{d}{d\eta} \left(\eta \frac{d\psi}{d\eta} \right) - i\frac{B}{2}\eta(1 - \eta^2)\psi - \frac{B^2}{4Pe^2}\eta\psi = 0,$$

$$\left. \frac{d\psi}{d\eta} \right|_{\eta=1} = 1, \quad \left. \frac{d\psi}{d\eta} \right|_{\eta=0} = 0. \quad (15)$$

An integration of the differential equation which appears in the boundary value problem expressed by Eq. (12) yields

$$\vartheta_0(\eta) = \gamma\eta^2 - \gamma\frac{\eta^4}{4} + C_0, \quad (16)$$

where C_0 is an integration constant.

It can be easily proved that the boundary conditions which appear in Eq. (12) are satisfied for any value of the integration constant C_0 .

The value of C_0 can be determined by considering the mixing-cup temperature of the fluid, defined as

$$T_m(x) = \frac{2}{\bar{u}r_0^2} \int_0^{r_0} [T(x, r)u(r) - \alpha \frac{\partial T(x, r)}{\partial x}] r dr. \quad (17)$$

The physical meaning of the mixing-cup temperature in forced convection problems with a relevant axial heat conduction in the fluid is widely discussed in the papers by Tamir and Taitel [16] and Barletta and Zanchini [14].

By employing the dimensionless mixing-cup temperature $\vartheta_m = k(T_m - T_c)/(q_0r_0)$, Eq. (17) can be rewritten in the dimensionless form

$$\vartheta_m(\xi) = 2 \int_0^1 \left[2(1 - \eta^2)\vartheta(\eta, \xi) - \frac{1}{Pe^2} \frac{\partial \vartheta(\eta, \xi)}{\partial \xi} \right] \eta d\eta. \quad (18)$$

The mixing-cup temperature of the fluid is related to the wall heat flux by the energy balance equation [14]

$$\frac{dT_m(x)}{dx} = \frac{2\alpha}{k\bar{u}r_0} q_w(x). \quad (19)$$

Since the inlet temperature is uniform with value T_e , by integrating Eq. (19) with respect to x in the interval $[-L, x]$, one obtains

$$T_m(x) - T_e = \frac{2\alpha q_0}{ukr_0} \left[\gamma(x+L) + \frac{\cos(\beta L) - \cos(\beta x)}{\beta} \right] \quad (20)$$

Eq. (20) can be rewritten in a dimensionless form

$$\vartheta_m(\xi) = 8\gamma(\xi - \xi_e) + \frac{8}{B} \cos(B\xi_e) - \frac{8}{B} \cos(B\xi), \quad (21)$$

where $\xi_e = -L/(2r_0Pe)$ is the dimensionless axial position of the inlet section. On the other hand, on account of Eqs. (8) and (18),

$$\begin{aligned} \vartheta_m(\xi) = & 8\gamma\xi + \vartheta_{0m} - \frac{8\gamma}{Pe^2} + \left[\vartheta_{1m} + \frac{2B}{Pe^2} \int_0^1 \vartheta_2(\eta)\eta \, d\eta \right] \\ & \times \sin(B\xi) + \left[\vartheta_{2m} - \frac{2B}{Pe^2} \int_0^1 \vartheta_1(\eta)\eta \, d\eta \right] \cos(B\xi). \end{aligned} \quad (22)$$

A comparison between Eqs. (21) and (22) yields

$$\vartheta_{0m} = \frac{8}{B} \cos(B\xi_e) - 8\gamma\xi_e + \frac{8\gamma}{Pe^2}. \quad (23)$$

As a consequence of Eqs. (16) and (18), ϑ_{0m} can be also written as

$$\vartheta_{0m} = \int_0^1 4\eta(1-\eta^2)\vartheta_0(\eta) \, d\eta = \frac{7}{24}\gamma + C_0. \quad (24)$$

Eqs. (23) and (24) yield

$$C_0 = \frac{8}{B} \cos(B\xi_e) - 8\gamma\xi_e + \frac{8\gamma}{Pe^2} - \frac{7}{24}\gamma. \quad (25)$$

By comparing Eqs. (16) and (25) with the expressions of $\vartheta_0(\eta)$ and C_0 in the limit $Pe \rightarrow \infty$ obtained in Ref. [15], one can conclude that the axial heat conduction in the fluid affects the axially-averaged dimensionless temperature only through the additive constant $8\gamma/Pe^2$ in the expression of C_0 . Obviously, this term vanishes in the case $\gamma = 0$.

On account of Eq. (15), $\psi(\eta)$ is a solution of the differential equation

$$\frac{d^2\psi}{d\eta^2} + \frac{1}{\eta} \frac{d\psi}{d\eta} - i\frac{B}{2} \left(1 - \frac{iB}{2Pe^2} - \eta^2 \right) \psi = 0. \quad (26)$$

The most general solution of Eq. (26) which fulfills the condition $d\psi(\eta)/d\eta|_{\eta=0} = 0$, i.e. which is finite at $\eta = 0$, can be expressed as [17]

$$\psi(\eta) = G(a, \omega) e^{-\omega\eta^2} {}_1F_1(a, 1; 2\omega\eta^2), \quad (27)$$

where $G(a, \omega)$ is an integration constant, ${}_1F_1$ is the confluent hypergeometric function and

$$A = 1 - \frac{iB}{2Pe^2}, \quad \omega = \sqrt{\frac{-iB}{8}}, \quad a = \frac{1 - \omega A}{2} \quad (28)$$

are complex dimensionless parameters.

The confluent hypergeometric function is defined as follows:

$${}_1F_1(s, t; z) = \frac{\Gamma(t)}{\Gamma(s)} \sum_{n=0}^{\infty} \frac{\Gamma(s+n)}{n! \Gamma(t+n)} z^n, \quad (29)$$

where Γ is Euler's gamma function. The most important properties of the confluent hypergeometric function ${}_1F_1$ are widely discussed in the textbook by Slater [18]. Recently, the confluent hypergeometric function has been employed by Piva [19,20] to analyze the laminar forced convection in circular ducts either with an exponential wall heat flux or with a relevant effect of wall axial conduction.

On account of Eqs. (27) and (28), the complex function $\psi(\eta)$ depends on Pe only through the parameter a .

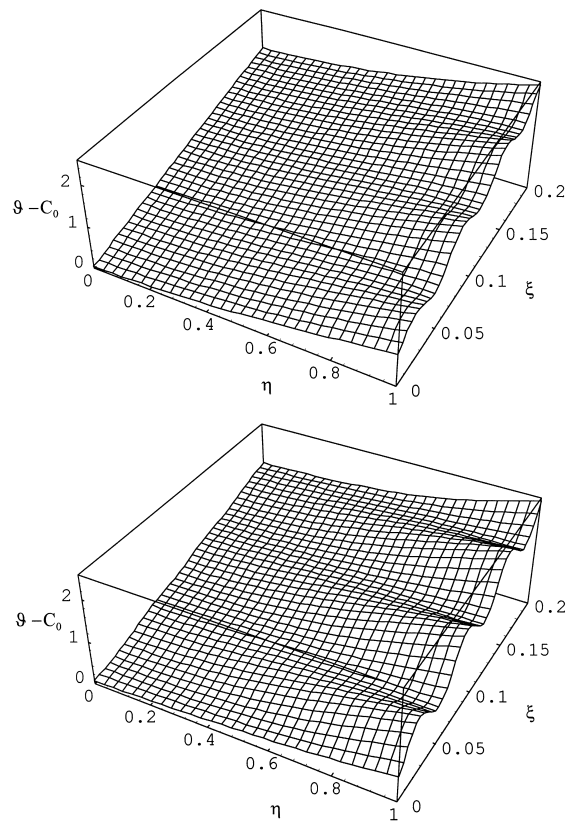


Fig. 1. Plots of $\vartheta - C_0$ vs. η and ξ for $\gamma = 1$ and $B = 100$, for $Pe = 10$ (upper frame) and 100 (lower frame).

The constant $G(a, \omega)$ can be determined by substituting Eq. (27) into the boundary condition which appears in Eq. (15), namely

$$1 = \left. \frac{d\psi(\eta)}{d\eta} \right|_{\eta=1} = 2G(a, \omega)\omega e^{-\omega} [2 {}_1F_1'(a, 1; 2\omega) - {}_1F_1(a, 1; 2\omega)], \quad (30)$$

where the derivative of the confluent hypergeometric function is given by [18]

$${}_1F_1'(s, t; z) = \frac{d}{dz} {}_1F_1(s, t; z) = \frac{s}{t} {}_1F_1(s + 1, t + 1; z). \quad (31)$$

Eqs. (30) and (31) yield

$$G(a, \omega) = \frac{e^\omega}{2\omega [2a {}_1F_1(a + 1, 2; 2\omega) - {}_1F_1(a, 1; 2\omega)]}. \quad (32)$$

In Figs. 1 and 2, three-dimensional plots of the dimensionless temperature field are presented. Both the plots reported in Fig. 1 refer to the case $\gamma = 1$ and $B = 100$ and have been drawn for two different values of the

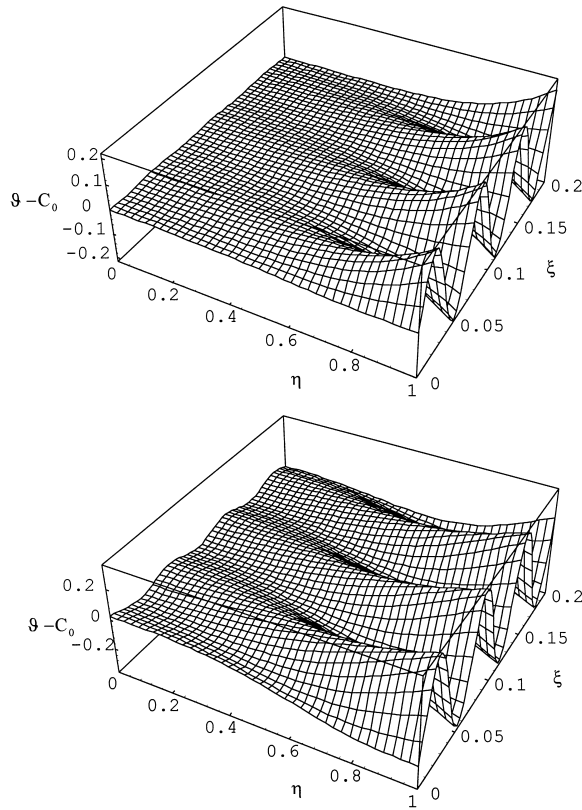


Fig. 2. Plots of $\vartheta - C_0$ vs. η and ξ for $\gamma = 0$ and $B = 100$, for $Pe = 10$ (upper frame) and 100 (lower frame).

Peclet number: $Pe = 10$ and 100 . The plots which appear in Fig. 2 refer to the case $\gamma = 0$, for the values of the parameters B and Pe considered in Fig. 1. It can be easily checked that the dimensionless temperature distributions for $Pe = 100$ are very close to those in the case $Pe \rightarrow \infty$, i.e. in the case of a negligible axial conduction. Both figures show that the amplitude of the temperature oscillations rapidly decreases moving from the wall to the axis of the duct. Moreover, the amplitude of the sinusoidal waves is significantly reduced when Pe decreases. The latter feature is emphasized in Fig. 3, where plots of the dimensionless wall temperature versus the dimensionless axial coordinate are reported. The plots have been drawn for $B = 100$ and for three different values of the Peclet number: $Pe = 1, 10$ and 100 . The plots in the top frame refer to the case $\gamma = 1$, while those in the bottom frame refer to the case $\gamma = 0$.

3. Local and fully developed Nusselt numbers

By employing the dimensionless temperature ϑ , the Nusselt number can be expressed as

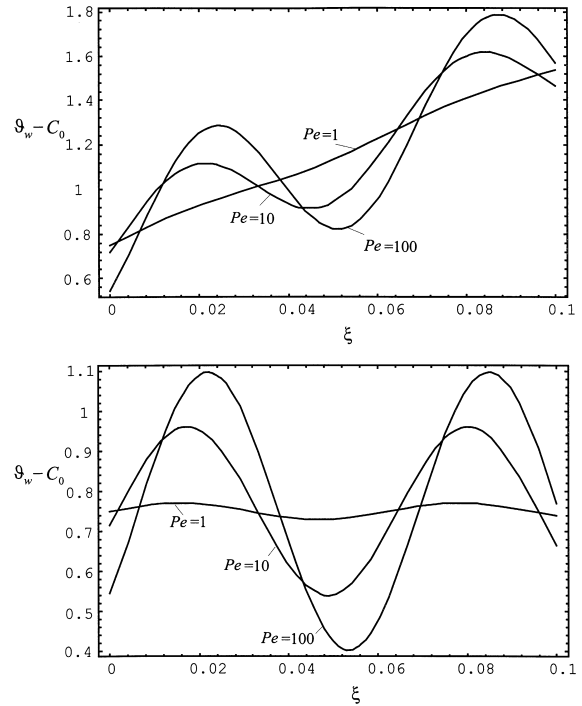


Fig. 3. Plots of $\vartheta_w - C_0$ vs. ξ for $B = 100$ and $Pe = 1, 10$ and 100 ; the upper frame refers to the case $\gamma = 1$, while the lower one refers to the case $\gamma = 0$.

Table 1
Values of $\vartheta_1(1)$ and $\vartheta_2(1)$ as functions of B , for $Pe = 0.5$ and 1

| B | $Pe = 0.5$ | | $Pe = 1$ | |
|-----|------------------|------------------------------|------------------|------------------------------|
| | $\vartheta_1(1)$ | $\vartheta_2(1) \times 10^6$ | $\vartheta_1(1)$ | $\vartheta_2(1) \times 10^6$ |
| 10 | 0.10542 | -264.78 | 0.22359 | -4579.6 |
| 20 | 0.051299 | -32.095 | 0.10541 | -529.39 |
| 30 | 0.033903 | -9.4218 | 0.069007 | -153.63 |
| 40 | 0.025319 | -3.9570 | 0.051299 | -64.189 |
| 50 | 0.020203 | -2.0206 | 0.040825 | -32.681 |
| 60 | 0.016807 | -1.1673 | 0.033903 | -18.843 |
| 70 | 0.014389 | -0.73418 | 0.028989 | -11.836 |
| 80 | 0.012579 | -0.49139 | 0.025319 | -7.9140 |
| 90 | 0.011173 | -0.34487 | 0.022473 | -5.5500 |
| 100 | 0.010050 | -0.25127 | 0.020203 | -4.0412 |
| 150 | 0.0066890 | -0.074323 | 0.013423 | -1.1932 |
| 200 | 0.0050125 | -0.031329 | 0.010050 | -0.50254 |
| 250 | 0.0040080 | -0.016032 | 0.0080322 | -0.25704 |
| 300 | 0.0033389 | -0.0092748 | 0.0066890 | -0.14865 |
| 350 | 0.0028612 | -0.0058393 | 0.0057307 | -0.093563 |
| 400 | 0.0025031 | -0.0039112 | 0.0050125 | -0.062657 |
| 450 | 0.0022247 | -0.0027465 | 0.0044544 | -0.043994 |
| 500 | 0.0020020 | -0.0020020 | 0.0040080 | -0.032064 |

$$Nu = \frac{2r_0q_w}{k(T_w - T_m)} = \frac{2[\gamma + \sin(B\xi)]}{\vartheta_w - \vartheta_m} \tag{33}$$

On account of Eqs. (8), (16), (21) and (25), $\vartheta_w - \vartheta_m$ is given by

$$\begin{aligned} \vartheta_w - \vartheta_m = & \left(\frac{11}{24} + \frac{8}{Pe^2} \right) \gamma + \vartheta_1(1) \sin(B\xi) \\ & + \left[\vartheta_2(1) + \frac{8}{B} \right] \cos(B\xi), \end{aligned} \tag{34}$$

where $\vartheta_1(1)$ and $\vartheta_2(1)$ can be evaluated, respectively, as the real and the imaginary part of $\psi(1)$ which, on account of Eqs. (27) and (32), can be expressed as

$$\psi(1) = \frac{{}_1F_1(a, 1; 2\omega)}{2\omega[2a {}_1F_1(a + 1, 2; 2\omega) - {}_1F_1(a, 1; 2\omega)]} \tag{35}$$

Values of $\vartheta_1(1)$ and $\vartheta_2(1)$ for B in the range $10 \leq B \leq 500$, obtained by employing Eq. (35), are reported in Table 1 for $Pe = 0.5, 1$ and in Table 2 for $Pe = 10, 100$. Tables 1 and 2 show that the amplitude of the dimensionless temperature oscillations at the wall, given by $\|\psi(1)\|$, is a decreasing function of B for a fixed value of Pe . Moreover, this decrease of $\|\psi(1)\|$ is steeper for smaller values of Pe .

On account of Eq. (34), Eq. (33) can be rewritten as

$$Nu =$$

$$\frac{2[\gamma + \sin(B\xi)]}{\left(\frac{11}{24} + \frac{8}{Pe^2} \right) \gamma + \vartheta_1(1) \sin(B\xi) + \left[\vartheta_2(1) + \frac{8}{B} \right] \cos(B\xi)} \tag{36}$$

The local Nusselt number is a periodic function of ξ with a period equal to $2\pi/B$. This function is free of singularities provided that the denominator on the right-hand side of Eq. (36) does not vanish, i.e. if the condition

$$\vartheta_1(1)^2 + \left[\vartheta_2(1) + \frac{8}{B} \right]^2 < \left[\left(\frac{11}{24} + \frac{8}{Pe^2} \right) \gamma \right]^2 \tag{37}$$

is fulfilled.

Let us first describe the behavior of the Nusselt number for $\gamma = 1$. If $\gamma = 1$, the condition expressed by Eq. (37) is certainly fulfilled for $B > 10^{-2}$. The precision of the calculus does not allow to find a lower value of B , which does not fulfil the inequality expressed by Eq. (37). However, one can assume that, if $\gamma = 1$, no singularities affect the local Nusselt number. In fact, for instance, if $r_0 = 1$ cm, the values $Pe = 10$ and $B = 10^{-2}$ correspond to an axial period of the wall heat flux $2\pi/\beta = 125.7$ m. Axial periods of this order of magnitude hardly allow one to attain, in practice, the condition of fully developed regime. In Figs. 4 and 5, plots of the local Nusselt number vs. the dimen-

Table 2
Values of $\vartheta_1(1)$ and $\vartheta_2(1)$ as functions of B , for $Pe = 10$ and 100

| B | $Pe = 10$ | | $Pe = 100$ | |
|-----|------------------|------------------------------|------------------|------------------|
| | $\vartheta_1(1)$ | $\vartheta_2(1) \times 10^3$ | $\vartheta_1(1)$ | $\vartheta_2(1)$ |
| 10 | 0.52313 | -809.57 | 0.45155 | -0.84301 |
| 20 | 0.48516 | -409.67 | 0.43171 | -0.47850 |
| 30 | 0.43828 | -267.34 | 0.40589 | -0.36985 |
| 40 | 0.39169 | -188.15 | 0.37956 | -0.31802 |
| 50 | 0.34916 | -136.42 | 0.35565 | -0.28577 |
| 60 | 0.31175 | -100.62 | 0.33509 | -0.26238 |
| 70 | 0.27939 | -75.263 | 0.31775 | -0.24400 |
| 80 | 0.25162 | -57.053 | 0.30315 | -0.22897 |
| 90 | 0.22784 | -43.829 | 0.29075 | -0.21637 |
| 100 | 0.20747 | -34.118 | 0.28009 | -0.20563 |
| 150 | 0.14029 | -11.696 | 0.24290 | -0.16898 |
| 200 | 0.10463 | -5.1054 | 0.21966 | -0.14692 |
| 250 | 0.083140 | -2.6326 | 0.20316 | -0.13153 |
| 300 | 0.068898 | -1.5235 | 0.19059 | -0.11984 |
| 350 | 0.058798 | -0.95758 | 0.18055 | -0.11046 |
| 400 | 0.051273 | -0.64008 | 0.17224 | -0.10266 |
| 450 | 0.045452 | -0.44860 | 0.16518 | -0.095974 |
| 500 | 0.040816 | -0.32642 | 0.15907 | -0.090134 |

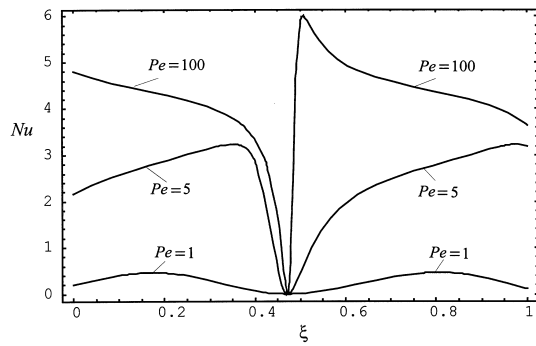


Fig. 4. Plots of Nu vs. ξ for $\gamma = 1$ and $B = 10$, for $Pe = 1, 5$ and 100 .

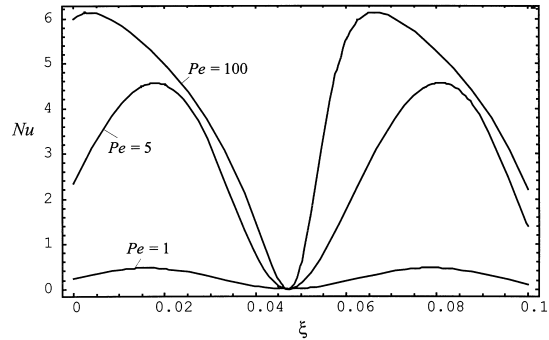


Fig. 5. Plots of Nu vs. ξ for $\gamma = 1$ and $B = 100$, for $Pe = 1, 10$ and 100 .

sionless axial coordinate are reported for three different values of Pe . The plots in Fig. 4 have been drawn for $B = 10$, while those in Fig. 5 have been drawn for $B = 100$. Both figures show that the amplitude of the oscillations of Nu reduces for decreasing values of Pe . Moreover, it can be easily verified that the plots of Nu vs. ξ in the case $Pe = 100$ are very similar to those in the case $Pe \rightarrow \infty$.

If no singularities arise, the mean value of the local Nusselt number is given by

$$\overline{Nu} = \frac{B}{2\pi} \int_0^{2\pi/B} Nu \, d\xi. \tag{38}$$

On account of Eq. (36), the integral on the right-hand side of Eq. (38) can be expressed as

$$\begin{aligned} \overline{Nu} = & \frac{2}{\sqrt{\left(\frac{11}{24} + \frac{8}{Pe^2}\right)^2 - \vartheta_1(1)^2 - \left[\vartheta_2(1) + \frac{8}{B}\right]^2}} \\ & \times \left(1 - \frac{\left(\frac{11}{24} + \frac{8}{Pe^2}\right)\vartheta_1(1)}{\vartheta_1(1)^2 + \left[\vartheta_2(1) + \frac{8}{B}\right]^2} \right) \\ & + \frac{2\vartheta_1(1)}{\vartheta_1(1)^2 + \left[\vartheta_2(1) + \frac{8}{B}\right]^2}. \end{aligned} \tag{39}$$

Values of the mean Nusselt number for $\gamma = 1$ are reported in Table 3 for different values of Pe and for B in the range $10 \leq B \leq 500$. Table 3 shows that for $Pe > 1$, the mean Nusselt number, if considered as a function of B , first decreases and then increases. The minimum is reached for different values of the parameter B , depending on the value assumed by the Peclet number. A comparison between the values reported in Table 3 and those reported in Ref. [15] shows that the values of \overline{Nu} for $Pe = 1000$ are almost equal to those

obtained in the case of negligible axial heat conduction ($Pe \rightarrow \infty$).

Let us now describe the behavior of the Nusselt number for $\gamma = 0$. If $\gamma = 0$, the inequality expressed by Eq. (37) is never fulfilled, so that the local Nusselt number is always affected by singularities. This means that, for every value of B and Pe , there exist axial positions where the wall temperature and the mixing-cup temperature are equal, while the wall heat flux does not vanish. The same behavior was found in the special case of negligible axial heat conduction $Pe \rightarrow \infty$ [15]. For every choice of the parameters B and Pe , the local Nusselt number is a function of ξ which becomes singular at the spatial positions $\xi = \xi_n$ for every integer n , where ξ_n is given by

$$\xi_n = -\frac{1}{B} \arctg\left(\frac{B\vartheta_2(1) + 8}{B\vartheta_1(1)}\right) + \frac{\pi n}{B}. \tag{40}$$

Fig. 6 presents plots of the local Nusselt number vs. the dimensionless axial coordinate for the case $\gamma = 0$ and $B = 100$. The upper frame refers to $Pe = 10$, while the lower frame refers to $Pe = 100$. On account of the singularities which affect the local Nusselt number, the integral which appears on the right-hand side of Eq. (38) is ill defined. However, its principal value exists and is given by

$$\overline{Nu} = \frac{2\vartheta_1(1)}{\vartheta_1(1)^2 + \left[\vartheta_2(1) + \frac{8}{B}\right]^2}. \tag{41}$$

The latter value can be employed to obtain the mean Nusselt number. Values of \overline{Nu} obtained by means of Eq. (41) are reported in Table 4, for different values of Pe and for B in the range $10 \leq B \leq 500$. The parameter \overline{Nu} significantly increases with B , especially for small values of Pe . A comparison between the values reported in Table 4 and those reported in Ref. [15]

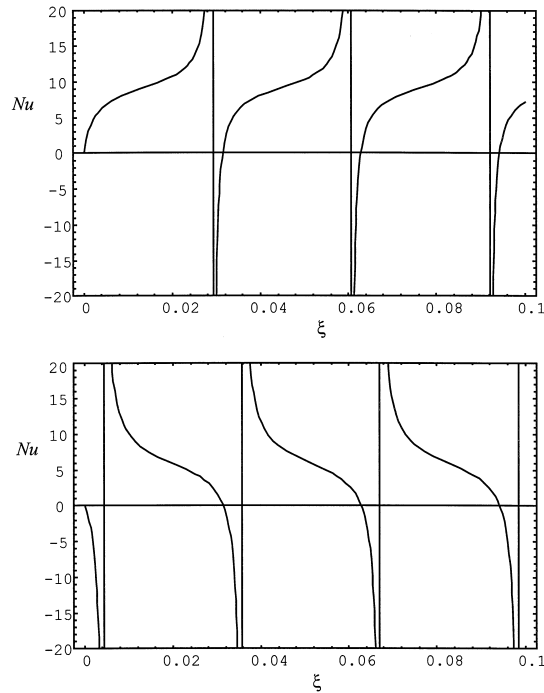


Fig. 6. Plots of Nu vs. ξ for $\gamma = 0$ and $B = 100$, for $Pe = 10$ (upper frame) and 100 (lower frame).

allows one to infer that for $Pe > 100$ the effects of axial conduction are very poor.

Let us now discuss the behavior of \overline{Nu} as a function of Pe , for a fixed value of B , both in the case $\gamma = 1$

Table 4
Values of \overline{Nu} in the case $\gamma = 0$, for B in the range $10 \leq B \leq 500$

| B | $Pe = 0.5$ | $Pe = 1$ | $Pe = 10$ | $Pe = 100$ | $Pe = 1000$ |
|-----|------------|----------|-----------|------------|-------------|
| 10 | 0.32401 | 0.65504 | 3.8219 | 4.3894 | 4.3961 |
| 20 | 0.63096 | 1.2351 | 4.1207 | 4.4844 | 4.4888 |
| 30 | 0.93843 | 1.8210 | 4.5633 | 4.6283 | 4.6291 |
| 40 | 1.2460 | 2.4081 | 5.1015 | 4.8047 | 4.8010 |
| 50 | 1.5536 | 2.9956 | 5.7020 | 4.9984 | 4.9895 |
| 60 | 1.8613 | 3.5834 | 6.3455 | 5.1977 | 5.1831 |
| 70 | 2.1689 | 4.1714 | 7.0214 | 5.3951 | 5.3743 |
| 80 | 2.4766 | 4.7594 | 7.7235 | 5.5864 | 5.5589 |
| 90 | 2.7843 | 5.3474 | 8.4477 | 5.7697 | 5.7349 |
| 100 | 3.0920 | 5.9355 | 9.1905 | 5.9446 | 5.9020 |
| 150 | 4.6304 | 8.8763 | 13.102 | 6.7124 | 6.6227 |
| 200 | 6.1688 | 11.817 | 17.201 | 7.3610 | 7.2117 |
| 250 | 7.7073 | 14.758 | 21.387 | 7.9389 | 7.7189 |
| 300 | 9.2457 | 17.699 | 25.617 | 8.4695 | 8.1688 |
| 350 | 10.784 | 20.640 | 29.871 | 8.9664 | 8.5755 |
| 400 | 12.323 | 23.582 | 34.140 | 9.4383 | 8.9482 |
| 450 | 13.861 | 26.523 | 38.418 | 9.8913 | 9.2934 |
| 500 | 15.340 | 29.464 | 42.703 | 10.330 | 9.6157 |

and in the case $\gamma = 0$. Plots of the mean Nusselt number vs. Pe are reported in Fig. 7. The plots in the upper frame refer to the case $\gamma = 1$ and have been drawn for $B = 250, 500, 750$ and 1000. The plots in the lower frame refer to the case $\gamma = 0$ and have been drawn for $B = 100, 200$ and 500. Fig. 7 shows that, for $\gamma = 1$, the mean Nusselt number reaches an absolute maximum for $Pe \cong 25$ if $B > 500$, a relative maximum for $Pe = 22$ if $B = 500$ and is a strictly increasing func-

Table 3
Values of \overline{Nu} in the case $\gamma = 1$, for B in the range $10 \leq B \leq 500$

| B | $Pe = 0.5$ | $Pe = 1$ | $Pe = 10$ | $Pe = 50$ | $Pe = 100$ | $Pe = 1000$ |
|-----|------------|----------|-----------|-----------|------------|-------------|
| 10 | 0.061536 | 0.23444 | 3.3684 | 4.1415 | 4.1741 | 4.1850 |
| 20 | 0.061574 | 0.23526 | 3.1841 | 4.0095 | 4.0482 | 4.0613 |
| 30 | 0.061587 | 0.23561 | 3.1027 | 3.9214 | 3.9639 | 3.9783 |
| 40 | 0.061595 | 0.23581 | 3.0796 | 3.8633 | 3.9083 | 3.9236 |
| 50 | 0.061599 | 0.23593 | 3.0873 | 3.8247 | 3.8715 | 3.8875 |
| 60 | 0.061602 | 0.23601 | 3.1101 | 3.7989 | 3.8471 | 3.8636 |
| 70 | 0.061604 | 0.23607 | 3.1395 | 3.7814 | 3.8308 | 3.8479 |
| 80 | 0.061606 | 0.23612 | 3.1708 | 3.7695 | 3.8200 | 3.8376 |
| 90 | 0.061607 | 0.23615 | 3.2018 | 3.7613 | 3.8129 | 3.8310 |
| 100 | 0.061608 | 0.23618 | 3.2313 | 3.7558 | 3.8083 | 3.8269 |
| 150 | 0.061611 | 0.23627 | 3.3479 | 3.7482 | 3.8046 | 3.8256 |
| 200 | 0.061613 | 0.23632 | 3.4229 | 3.7534 | 3.8120 | 3.8351 |
| 250 | 0.061614 | 0.23634 | 3.4732 | 3.7633 | 3.8215 | 3.8466 |
| 300 | 0.061614 | 0.23636 | 3.5090 | 3.7751 | 3.8312 | 3.8580 |
| 350 | 0.061615 | 0.23637 | 3.5357 | 3.7880 | 3.8405 | 3.8686 |
| 400 | 0.061615 | 0.23638 | 3.5563 | 3.8017 | 3.8492 | 3.8785 |
| 450 | 0.061615 | 0.23639 | 3.5726 | 3.8159 | 3.8574 | 3.8876 |
| 500 | 0.061616 | 0.23640 | 3.5859 | 3.8305 | 3.8652 | 3.8960 |

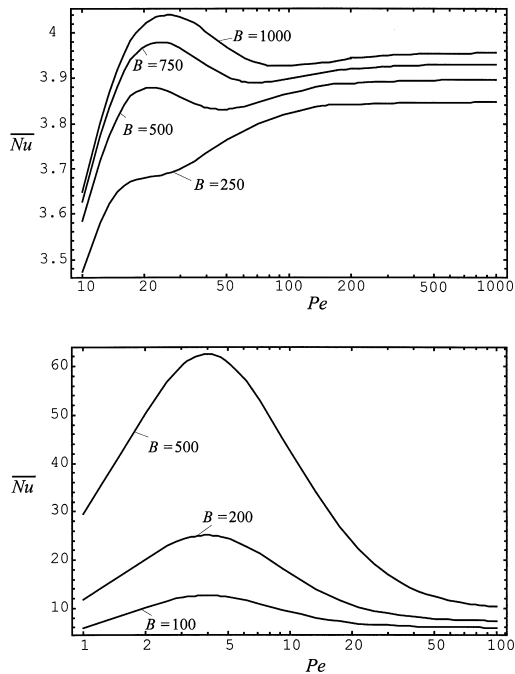


Fig. 7. Plots of \overline{Nu} vs. Pe . The plots in the upper frame have been drawn for $\gamma = 1$ and for $B = 250, 500, 750$ and 1000 . The plots in the lower frame have been drawn for $\gamma = 0$ and for $B = 100, 200$ and 500 .

tion of Pe if $B = 250$. The same figure reveals that, for $\gamma = 0$, the mean Nusselt number reaches a maximum for $Pe \cong 4$ and that the position of this maximum is almost independent of the value assumed by B . For instance, for a duct with radius 5 mm, $Pe = 4$ and $B = 100$ correspond to an axial period of the wall heat flux $2\pi/\beta \cong 2.5$ mm. On the other hand, $Pe = 25$ and $B = 1000$ correspond, for the same duct, to an axial period $2\pi/\beta \cong 1.6$ mm.

Finally, let us discuss the behavior of the local convection coefficient h in a special case. Let us consider mercury flowing in a circular duct with radius $r_0 = 5$ mm and a wall heat flux distribution with $\beta = 10 \text{ m}^{-1}$. The thermophysical properties of mercury at 20°C are the following [21]: $k = 9.304 \text{ W/(m K)}$, $\alpha = 4.941 \times 10^{-6} \text{ m}^2/\text{s}$, $\nu = 1.147 \times 10^{-7} \text{ m}^2/\text{s}$. The convection coefficient can be easily evaluated by employing Eq. (36). Plots of the convection coefficient h vs. the axial coordinate x are reported in Figs. 8 and 9 for $\bar{u} = 0.022$ and 0.006 m/s . As it can be easily verified, the values of mean velocity considered in this example are such that the flow regime of mercury is laminar. Fig. 8 refers to the case $\gamma = 1$, while Fig. 9 refers to the case $\gamma = 0$. In Fig. 9, the upper frame has been drawn for $\bar{u} = 0.006 \text{ m/s}$, while the lower frame for $\bar{u} = 0.022 \text{ m/s}$. As expected, both Figs. 8 and 9 show

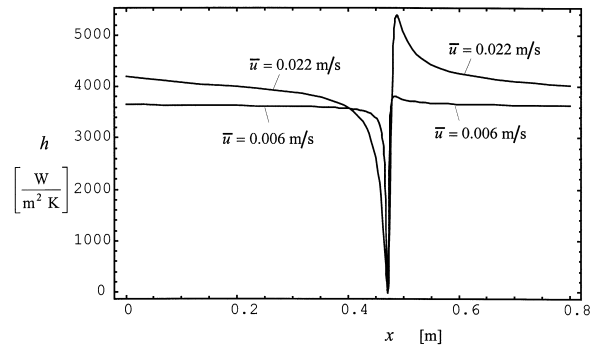


Fig. 8. Plots of h vs. x for mercury in the case $\gamma = 1$. The plots have been drawn for $r_0 = 5 \text{ mm}$, $\beta = 10 \text{ m}^{-1}$, and refer to $\bar{u} = 0.006$ and 0.022 m/s .

that the convection coefficient in the case $\bar{u} = 0.022 \text{ m/s}$ is generally higher than that in the case $\bar{u} = 0.006 \text{ m/s}$. Fig. 8 reveals that, independently of the choice of \bar{u} , the convection coefficient collapses to zero for $x = 0.471$. In fact, on account of Eq. (33), one can easily infer that, for $\gamma = 1$, the convection coefficient vanishes whenever $\sin(\beta x) = -1$. Finally, Fig. 9 shows that a slight difference in the position of the singularities occurs between the cases $\bar{u} = 0.006$ and 0.022 m/s .

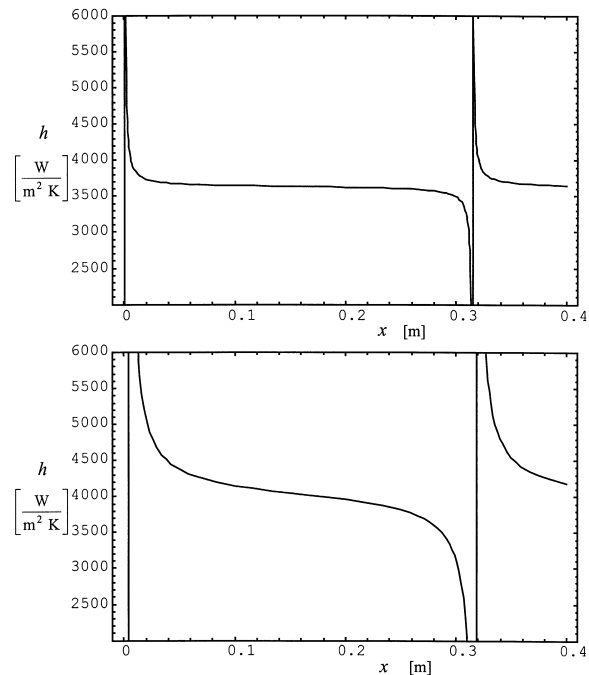


Fig. 9. Plots of h vs. x for mercury in the case $\gamma = 0$. The plots have been drawn for $r_0 = 5 \text{ mm}$ and $\beta = 10 \text{ m}^{-1}$. The upper frame refers to $\bar{u} = 0.006 \text{ m/s}$ and the lower frame to $\bar{u} = 0.022 \text{ m/s}$.

4. Conclusions

The effects of axial heat conduction in the fluid have been investigated for laminar forced convection in an infinitely long circular duct. A boundary condition given by a sinusoidally varying axial distribution of heat flux has been considered. Reference has been made to the hydrodynamically developed flow. The thermally developed region, where the temperature distribution can be expressed as the sum of a linear function and a periodic function of the axial coordinate, has been studied.

Two different boundary conditions have been analyzed: (a) a sinusoidal wall heat flux such that the modulus of the mean value is equal to the amplitude, (b) a sinusoidal wall heat flux with a vanishing mean value. An analytical evaluation of the temperature field and of the local Nusselt number has been performed. In particular, these quantities have been expressed in terms of the confluent hypergeometric function. The behavior of the temperature distribution has been compared with that obtained by neglecting axial heat conduction in the fluid. Indeed, for small values of the Peclet number, the amplitude of the sinusoidal waves is significantly reduced and the amplitude of the temperature oscillations undergoes a steeper decrease moving from the wall to the axis of the duct.

It has been shown that, in case (a), no singularities affect the local Nusselt number. On the other hand, in case (b), singularities arise for any value of B and Pe . The occurrence of these singularities is due the existence of axial positions where the wall temperature and the mixing-cup temperature assume the same value, while the wall heat flux is nonzero.

The mean Nusselt number in an axial period has been obtained and, whenever singularities are present, this quantity has been evaluated as the principal value of an integral. Moreover, the mean Nusselt number has been plotted as a function of the Peclet number for fixed values of B , in both case (a) and case (b). The plots reveal that, in case (a), the mean Nusselt number reaches an absolute maximum for $Pe \cong 25$, provided that B is higher than 500. On the other hand, in case (b), the mean Nusselt number reaches a maximum for $Pe \cong 4$, independently of the value assumed by B .

References

- [1] R.K. Shah, A.L. London, Laminar flow forced convection in ducts. *Advances in Heat Transfer*, Supplement 1, Academic Press, New York, 1978.
- [2] W.M. Kays, H.C. Perkins, Forced convection, internal flow in ducts, in: W.M. Rosenhow, J.P. Hartnett, E.N. Ganic (Eds.), *Handbook of Heat Transfer*

- Fundamentals*, McGraw-Hill, New York, 1985 (Chapter 7).
- [3] R.K. Shah, M.S. Bhatti, Laminar convective heat transfer in ducts, in: S. Kakaç, R.K. Shah, W. Aung (Eds.), *Handbook of Single Phase Convective Heat Transfer*, Wiley, New York, 1987 (Chapter 3).
- [4] H.M. Soliman, Analysis of low Peclet heat transfer during slug flow in tubes with axial wall conduction, *ASME Journal of Heat Transfer* 106 (1984) 782–788.
- [5] M.A. Ebadian, H.Y. Zhang, An exact solution of extended Graetz problem with axial heat conduction, *International Journal of Heat and Mass Transfer* 32 (1989) 1709–1717.
- [6] M.A. Ebadian, H.Y. Zhang, Effects of heat generation and axial heat conduction in laminar flow inside a circular pipe with a step change in wall temperature, *International Communications in Heat and Mass Transfer* 17 (1990) 621–635.
- [7] X. Yin, H.H. Bau, The conjugate Graetz problem with axial conduction, *ASME Journal of Heat Transfer* 118 (1996) 482–485.
- [8] S. Olek, Heat transfer in duct flow of non-Newtonian fluids with axial conduction, *International Communications in Heat and Mass Transfer* 25 (1998) 929–938.
- [9] A. Faghri, M.M. Chen, E.T. Mahefkey, Simultaneous axial conduction in the fluid and in the pipe wall for forced convective laminar flow with blowing and suction at the wall, *International Journal of Heat and Mass Transfer* 32 (1989) 281–288.
- [10] T.V. Nguyen, Laminar heat transfer for thermally developing flow in ducts, *International Journal of Heat and Mass Transfer* 35 (1992) 1733–1741.
- [11] S. Bilir, Numerical solution of Graetz problem with axial conduction, *Numerical Heat Transfer A* 21 (1992) 493–500.
- [12] S. Bilir, Laminar flow heat transfer in pipes including two-dimensional wall and fluid axial conduction, *International Journal of Heat and Mass Transfer* 38 (1995) 1619–1625.
- [13] A.J. Pearlstein, B.P. Dempsey, Low Peclet number heat transfer in a laminar tube flow subjected to axially varying wall heat flux, *ASME Journal of Heat Transfer* 110 (1988) 796–798.
- [14] A. Barletta, E. Zanchini, On the laminar forced convection with axial conduction in a circular tube with exponential wall heat flux, *Heat and Mass Transfer* 30 (1995) 283–290.
- [15] A. Barletta, E. Zanchini, Laminar forced convection with sinusoidal wall heat flux distribution: axially periodic regime, *Heat and Mass Transfer* 31 (1995) 41–48.
- [16] A. Tamir, Y. Taitel, On the concept of the “mixing cup” temperature in flows with axial conduction, *The Canadian Journal of Chemical Engineering* 50 (1972) 421–424.
- [17] H.A. Lauwerier, The use of confluent hypergeometric functions in mathematical physics and the solution of an eigenvalue problem, *Applied Scientific Research A* 2 (1951) 184–204.
- [18] L.J. Slater, *Confluent Hypergeometric Functions*, Cambridge University Press, Cambridge, UK, 1960.

- [19] S. Piva, An analytical approach to fully developed heating of laminar flows in circular pipes, *International Communications in Heat and Mass Transfer* 22 (1995) 815–824.
- [20] S. Piva, Axial wall conduction preheating effects in high Peclet number laminar forced convection, *International Journal of Heat and Mass Transfer* 39 (1996) 3511–3517.
- [21] K. Raznjevic, *Handbook of Thermodynamic Tables*, 2nd ed., Begell House, New York, 1995.